

ORIGINAL ARTICLE

CircRNA circ_0008037 facilitates tumor growth and the Warburg effect via upregulating NUCKS1 by binding to miR-433-3p in non-small cell lung cancer

Jia Yu[†] | Haining Zhang[†] | Chunsheng Zhao | Guanghui Li | Yingying Zhang | Yang Sun[✉]

Department of Respiratory, Dongying People's Hospital, Dongying, China

Correspondence

Yang Sun, Department of Respiratory, Dongying People's Hospital, No.317, Nanyi Road, Dongying, Shandong, China Dongying 257091, Shandong, China.

Email: gzyyx1026@163.com

Abstract

Background: Circular RNAs (circRNAs) participate in the genesis and progression of tumors, including non-small cell lung cancer (NSCLC). At present, the role and regulatory mechanisms of circRNAs in NSCLC have not been fully elucidated. The aim of this study was to explore the role and regulatory mechanism of circRNA hsa_circ_0008037 (circ_0008037) in NSCLC.

Methods: Expression of circ_0008037 in NSCLC tissues and cells was detected by quantitative real-time polymerase chain reaction (RT-qPCR). Loss-of-function experiments were performed to analyze the influence of circ_0008037 knockdown on proliferation, migration, invasion, and the Warburg effect of NSCLC cells. Western blotting was utilized for protein analysis. The regulatory mechanism of circ_0008037 was surveyed by bioinformatics analysis, RNA pull-down assay, and dual-luciferase reporter assay. Xenograft assay was used to validate the oncogenicity of circ_0008037 in NSCLC in vivo.

Results: Circ_0008037 was upregulated in NSCLC tissues and cells. Circ_0008037 downregulation reduced tumor growth in vivo and repressed proliferation, migration, invasion, and decreased the Warburg effect of NSCLC cells in vitro. Mechanically, circ_0008037 regulated nuclear ubiquitous casein kinase and cyclin-dependent kinase substrate 1 (NUCKS1) expression via sponging miR-433-3p. Furthermore, MiR-433-3p inhibitor reversed the inhibiting influence of circ_0008037 silencing on proliferation, migration, invasion, and the Warburg effect of NSCLC cells. Also, NUCKS1 elevation overturned the repressive influence of miR-433-3p mimic on proliferation, migration, invasion, and the Warburg effect of NSCLC cells.

Conclusion: Circ_0008037 accelerated tumor growth and elevated the Warburg effect via regulating NUCKS1 expression by adsorbing miR-433-3p, providing an underlying target for NSCLC treatment.

KEYWORDS

circ_0008037, miR-433-3p, NSCLC, NUCKS1

INTRODUCTION

Non-small cell lung cancer (NSCLC) is the main subtype of lung cancer.¹ The 5-year survival rate of NSCLC patients is less than 20% as a result of metastasis and relapse.² Due to

the lack of early symptoms, approximately 50% of NSCLC patients are already in stage IV at the time of diagnosis.³ Therefore, understanding the molecular mechanism of NSCLC is of great significance.

Under physiological oxygen conditions, tumor cells increase the utilization of glycolysis to meet their energy requirements instead of oxidative phosphorylation, which is

[†]Jia Yu and Haining Zhang contribute to this work equally as co-first authors.

the Warburg effect.⁴ Increased glycolysis will produce large amounts of lactate, leading to acidification of the extracellular pH in the tumor microenvironment.⁵ However, this acidosis is conducive to metastasis, angiogenesis, and immunosuppression.⁶ Therefore, exploring the mechanism that affects the Weinberg effect is crucial in NSCLC progression.

Circular RNAs (circRNAs) are formed by multiple exons or a single exon through reverse splicing.⁷ It has been reported that circRNAs can regulate gene expression via binding to microRNAs (miRs).⁸ CircRNAs take part in a wide range of pathophysiological processes due to their specificity, abundance, and conservation.⁹ For instance, circRNA circ_HMCU contributed to breast cancer progression via sponging the let-7 family.¹⁰ MiRs are small endogenous RNAs that maintain cell homeostasis through negatively regulating gene expression.^{11,12} An increasing number of studies have proved that miRs serve as oncomiRs or tumor suppressors in diverse cancers.¹² For example, miR-615-3p exerts a carcinogenic role in breast cancer¹³ while playing a tumor-inhibiting role in NSCLC.¹⁴ Recent studies have exposed the inhibitory effect of miR-433-3p on NSCLC progression.¹⁵⁻¹⁷ However, the dysregulation of miR-433-3p in NSCLC has not been fully explained.

NUCKS1, a chromatin-related multifunctional protein, serves as a key transcriptional regulator of various signaling pathways.¹⁸ It has a potential role in glucose metabolism.¹⁹ Also, NUCKS1 acts as an independent risk factor for colorectal cancer recurrence.²⁰ Recent studies have revealed that NUCKS1 act as an oncogene in gastric cancer,²¹ hepatocellular carcinoma,²² and NSCLC.²³ However, the regulatory network related to NUCKS1 in NSCLC is still indistinct.

Ubiquitin-like modifier activating enzyme 2 (UBA2) plays a critical role in NSCLC cell proliferation.²⁴ Through circinteractome, we discovered that circRNA hsa_circ_0008037 (circ_0008037) from the UBA2 gene was expressed at A549 cells. Nevertheless, the function of circ_0008037 in NSCLC is unclear. Herein, the function and regulatory mechanism of circ_0008037 in NSCLC were surveyed.

METHODS

Tissue specimens

The research was ratified by the Ethics Committee of Dongying People's Hospital. Fifty-six paired NSCLC tissue specimens and paracarcinoma tissue specimens were collected from Dongying People's Hospital. None of radiotherapy or chemotherapy was administrated prior to surgical excision. All patients provided their written informed consent. The clinicopathological characteristics of NSCLC patients are shown in Table 1.

Cell culture and transfection

A549 cells (CL-0016, Procell) and H1975 cells (CL-0298, Procell), as well as human bronchial epithelial cells BEAS-2B

TABLE 1 Correlation between hsa_circ_0008037 expression and clinicopathological characteristics in NSCLC patients ($n = 56$)

Clinicopathological parameters	hsa_circ_0008037 expression			p-value ^a
	Case	Low ($n = 28$)	High ($n = 28$)	
Gender				0.4151
Male	33	18	15	
Female	23	10	13	
Age (years)				0.2838
≤55	30	17	13	
>55	26	11	15	
Tumor size				0.0156*
≤3 cm	25	17	8	
>3 cm	31	11	20	
TNM stage				0.0257*
I–II	20	14	6	
III	36	14	22	
Lymphatic metastasis				0.0221*
Negative	18	13	5	
Positive	38	15	23	

^aChi-square test.

* $P < 0.05$.

(CL-0496, Procell), were cultured in Roswell Park Memorial Institute-1640 medium (Sigma) supplemented with fetal bovine serum (10%, Solarbio) and streptomycin/penicillin (1%, Solarbio).

Transfection of NSCLC cells was executed by using Lipofectamine 3000 reagent (Invitrogen). siRNA targeting circ_0008037 (si-circ_0008037) and matched negative control (si-NC), miR-433-3p inhibitor and mimic (anti-miR-433-3p and miR-433-3p), as well as corresponding controls (anti-miR-NC and miR-NC), were synthesized by Genechem. The pcDNA3.1-NUCKS1 (NUCKS1) vectors were constructed using the empty pcDNA3.1 vector (vector) (Invitrogen). Sequences for siRNAs are shown in Table S1.

RNA isolation and real-time quantitative polymerase chain reaction (RT-qPCR)

Isolation of total RNA from tissue and cells was performed using the miRNeasy Mini Kit (Qiagen). Isolation of nuclear and cytoplasmic RNAs from NSCLC cells was executed using the PARIS Kit (Invitrogen). Reverse transcription was executed using Reverse Transcription Kits (Vazyme), followed by execution of qPCR with the SYBR Green PCR Master Mix (Bio-Rad) and specific primers (Table 2). Expression was quantified using the $2^{-\Delta\Delta CT}$ method and β -actin or U6 acted as reference genes.

Actinomycin D (ActD) and RNase R treatment

For ActD treatment, NSCLC cells were cultured in a complete medium supplemented with ActD (2 μ g/ml) to prevent

TABLE 2 Primer sequences for RT-qPCR

Genes	Primer sequences (5'-3')
β -actin	Forward (F): 5'-TGGATCAGCAAGCAGGAGTA-3' Reverse (R): 5'-TCGGCCACATTGTGAACTTT-3'
circ_0008037	F: 5'-CTGCCCGAAACCATGTTAAT-3' R: 5'-TCAGGGTTCATGATGCTGTC-3'
UBA2	F: 5'-AGAGGTGACTGTGCGGCTGAAT-3' R: 5'-GGACATCTGGTGCTACCATAGC-3'
NUCKS1	F: 5'-GACGATAGTACTATGGCAGTTC-3' R: 5'-CCTTTCCTGGACTTGGCGTCA-3'
miR-433-3p	F: 5'-GCGATCATGATGGGCTCCT-3' R: 5'-AGTGCAGGGTCCGAGGTATT-3'
U6	F: 5'-CTCGCTTCGGCAGCAC-3' R: 5'-AACGCTTCACGAATTTGCGT-3'

RNA transcription. For RNase R digestion, the extracted RNA from NSCLC cells was digested using 3 U/ μ g RNase R (Solarbio). Thereafter, the abundance of circ_0008037 and UBA2 mRNA was evaluated with RT-qPCR.

Cell proliferation assessment

Cell proliferation was evaluated with MTT and colony formation assays. For the MTT assay, NSCLC cells (200 μ l, 1×10^4 cells/ml) were incubated in 96-well plates. Next, the MTT solution (20 μ l, Sigma) was added into each well and the purple crystals were dissolved with dimethylsulfoxide (150 μ l, Sigma). The absorbance was then measured with a Microplate Reader (Bio-Rad) at 570 nm. For the colony formation assay, NSCLC cells (2×10^3 cells/well) were seeded into 6-well plates and cultured for 2 weeks, followed by staining with crystal violet (0.5%, Solarbio). The colonies were counted using a light microscope (Olympus).

Cell migration and invasion assay

The transwell chambers (Costar) were utilized for migration and invasion analysis. The difference between the migration assay and the invasion assay was that the upper chamber used for the invasion assay was precoated with Matrigel (Sigma). In brief, the lower chamber was supplemented with RPMI-1640 medium containing FBS (10%) (500 μ l), and the upper chamber was added with serum-free RPMI-1640 medium (200 μ l) containing NSCLC cells (200 μ l, 5×10^4 cells/ml). After dyeing with crystal violet (0.5%, Beyotime), the migrating and invading cells were counted under a microscope (Olympus).

Evaluation of glycolysis

Lactate production and glucose consumption were assessed with a lactate assay kit (Solarbio) or glucose assay kit

(Solarbio) according to the manufacturer's instructions. The ECAR and OCR of transfected NSCLC cells were evaluated by using an XFe 96 Extracellular Flux analyzer (Seahorse Bioscience) with an XF glycolysis stress test Kit (Seahorse Bioscience) or XF Cell Mito Stress Test Kit (Seahorse Bioscience) according to the manufacturer's instructions.

Western blotting

Extraction of total protein was executed using the RIPA lysis buffer (Beyotime), and western blotting was executed as previously described.²⁵ Antibodies used in the study were as follows: matrix metalloproteinase 2 (MMP2) (ab97779, 1:2000, Abcam), matrix metalloproteinase 9 (MMP9) (ab228402, 1:1000, Abcam), hexokinase 2 (HK2) (ab227198, 1:10000, Abcam), lactate dehydrogenase A (LDHA) (ab125683, 1:1000, Abcam), and NUCKS1 (PA5-26535, 1:1000, Invitrogen), anti- β -actin (ab115777, 1:200, Abcam), and goat anti-rabbit IgG (ab6721, 1:10000, Abcam). Protein bands were visualized with enhanced chemiluminescence solution (Beyotime).

RNA pulldown assay

The biotinylated (Biotin)-miR-433-3p-WT and Biotin-433-3p-MUT probes (Genechem) were incubated with M-280 streptavidin magnetic beads (Invitrogen) to establish probe-coated beads, respectively. Next, the probe-coated beads were coincubated with the lysates of NSCLC cells. The abundance of circ_0008037 and GAPDH in the RNA complexes was detected with RT-qPCR.

Dual-luciferase reporter assay

The sequences of wild type circ_0008037 (circ_0008037 WT), mutant circ_0008037 (circ_0008037 MUT), wild type 3' untranslated regions (UTR) of NUCKS1 (NUCKS1 3'-UTR-WT), and mutant 3'UTR of NUCKS1 (NUCKS1 3'-UTR-MUT) were inserted into the psiCHECK-2 vector (Promega), respectively. Then, the luciferase reporter vectors carrying circ_0008037 WT, circ_0008037 MUT, NUCKS1 3'-UTR-WT, or NUCKS1 3'-UTR-MUT were transfected into NSCLC cells along with miR-NC or miR-433-3p. The luciferase activities were determined with the luciferase reporter assay kit (Promega).

Xenograft assay

For xenograft assay, BALB/c nude mice (Vital River, Beijing, China) (five mice/group) were subcutaneously injected with about 2×10^6 cells A549 cells stably expressing sh-circ_0008037 or sh-NC. Tumor volume was measured once a week. Five weeks later, the mice were sacrificed by cervical

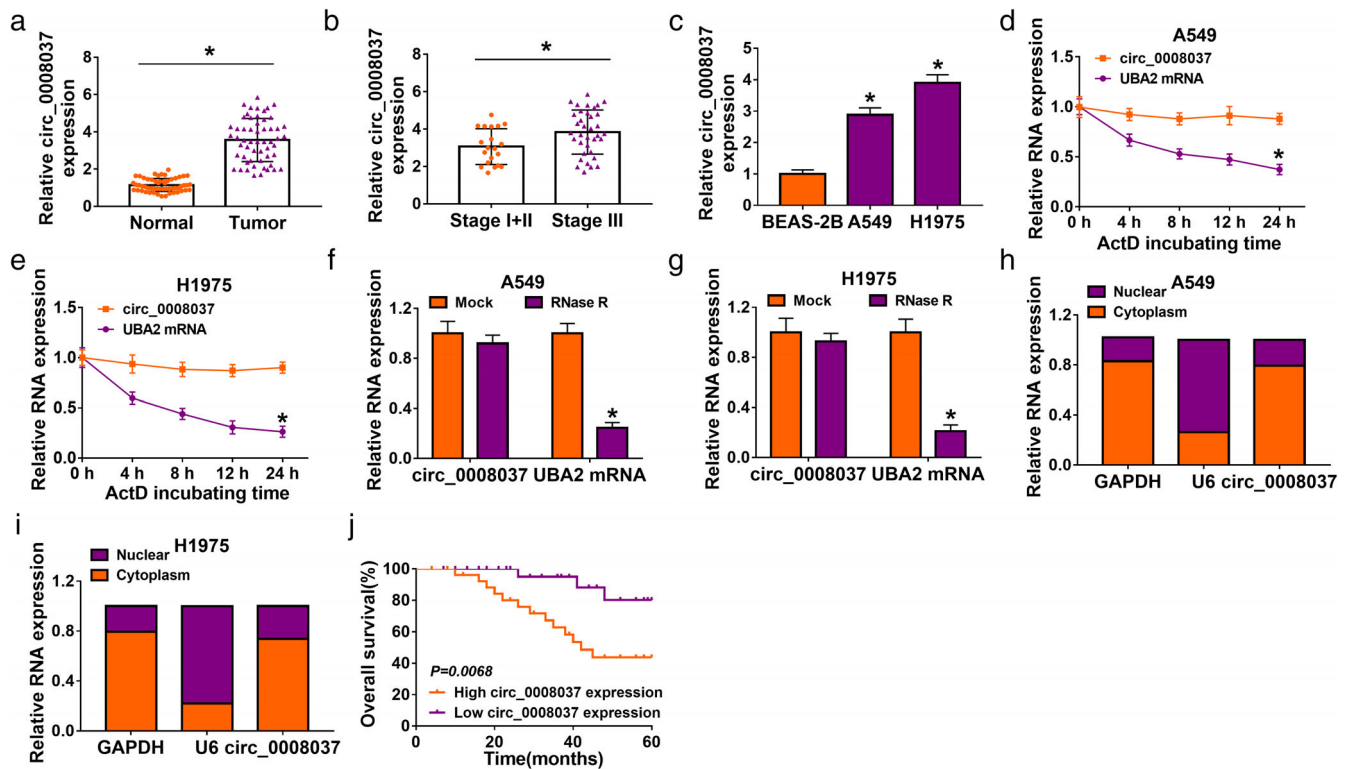


FIGURE 1 Circ_0008037 was overexpressed in NSCLC. (a) RT-qPCR analysis of circ_0008037 in 56 paired NSCLC tissues and paracarcinoma tissues. (b) RT-qPCR analysis of circ_0008037 in NSCLC tissues at stages I + II and III. (c) RT-qPCR assessment of circ_0008037 in A549, H1975, and BEAS-2B cells. (d–g) After ActD or RNase R treatment, the levels of circ_0008037 and UBA2 were evaluated by RT-qPCR. (h, i) After cytoplasm RNA and nuclear RNA isolation, the levels of GAPDH, U6, and circ_0008037 were assessed with RT-qPCR. (j) Kaplan–Meier survival analysis indicated that circ_0008037 expression was correlated with a worse patient prognosis. Log-rank test was used to estimate the significance. * $P < 0.05$

dislocation under isoflurane (5%). Tumors volume was calculated following the equation: Volume = (length \times width²)/2. Immunohistochemistry (IHC) was conducted following the methods described previously,²⁶ and a primary antibody against Ki67 (ab92742, 1:500, Abcam) was used for IHC analysis. The protocols of xenograft assay were authorized by the Animal Ethics Committee of Dongying People's Hospital.

Statistical analysis

Data from three biological replicates were exhibited as the mean \pm standard deviation. Student's *t*-test or ANOVA was utilized for comparison of between two groups or more than two groups. Analysis of data was implemented using GraphPad Prism 6 software (GraphPad). Statistical significance was indicated as follows: * $P < 0.05$.

RESULTS

Circ_0008037 was overexpressed in NSCLC

To validate changes in circ_0008037 expression in NSCLC, we performed RT-qPCR analysis using RNA isolated from

NSCLC tissues and paracarcinoma tissues. The results exhibited that circ_0008037 was highly expressed in NSCLC tissues compared to that in paired paracarcinoma tissues (Figure 1a). Similarly, circ_0008037 was highly expressed in NSCLC patients with stage III when compared to that in NSCLC patients with stage I + II (Figure 1b). Furthermore, high circ_0008037 expression was related to tumor size, TNM stage, and lymphatic metastasis of NSCLC patients (Table 1). Furthermore, circ_0008037 expression was higher in NSCLC cells than that in BEAS-2B cells (Figure 1c). Also, ActD (a known RNA polymerase inhibitor) treatment observably decreased the half-life of liner UBA2 compared to circ_0008037 in NSCLC cells (Figure 1d,e). Furthermore, RNase R (a known exoribonuclease) treatment resulted in a marked decrease in UBA2 mRNA expression but had no effect on circ_0008037 expression (Figure 1f,g). These stable properties supported the circular structure of circ_0008037. We also analyzed the localization of circ_0008037 in NSCLC cells. Results presented that circ_0008037 was preferentially distributed in the cytoplasm of NSCLC cells (Figure 1h,i). The correlation between circ_0008037 expression and prognosis was analyzed by log-rank test. As displayed in Figure 1j, high circ_0008037 expression predicted a worse prognosis in a cohort of 56 NSCLC patients. Collectively, these results manifested that circ_0008037 was upregulated in NSCLC and its upregulation might be related to NSCLC progression.

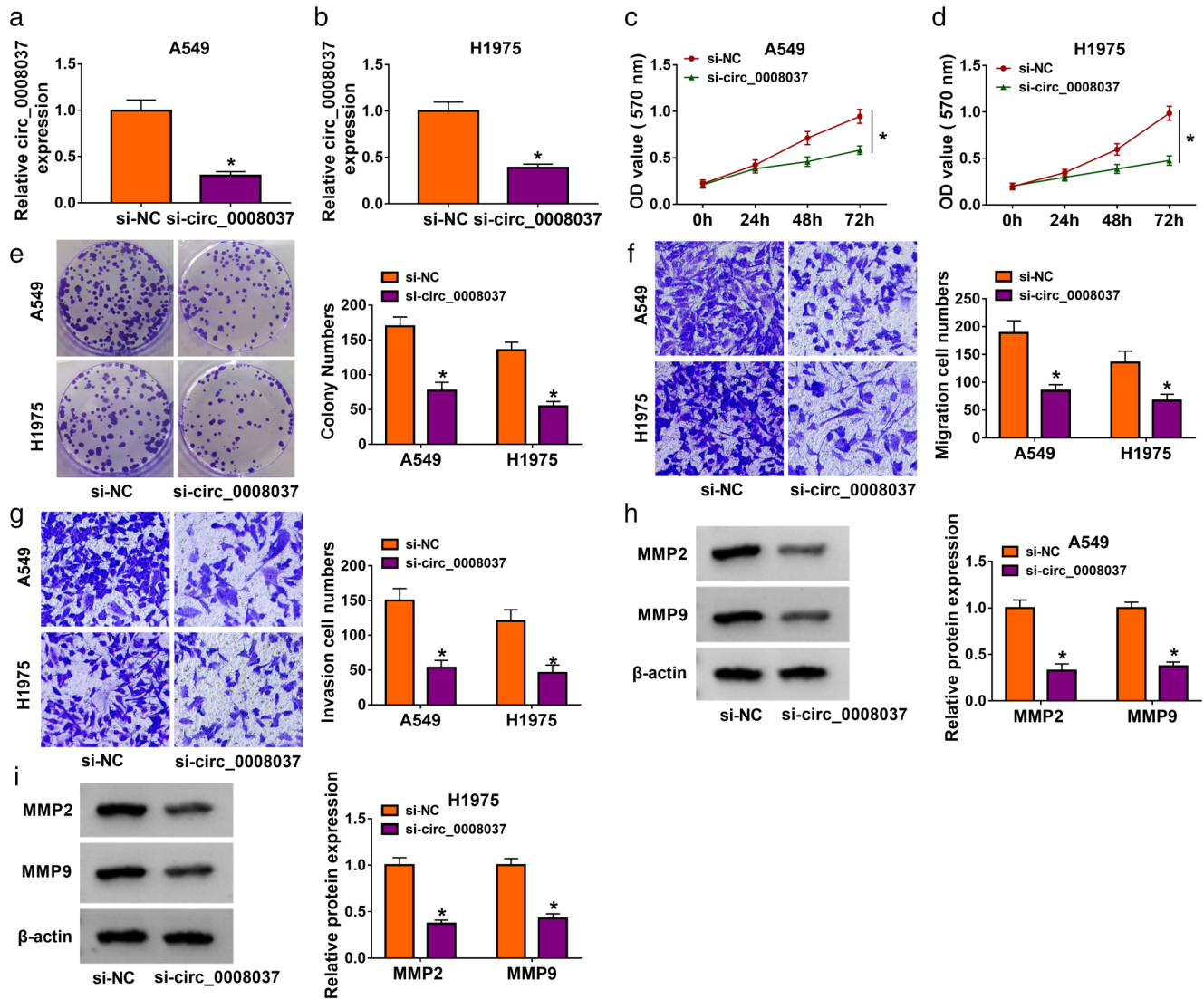


FIGURE 2 Effects of circ_0008037 silencing on proliferation, migration, and invasion of NSCLC cells. (a–i) NSCLC cells were transfected with si-circ_0008037 or si-NC. (a, b) RT-qPCR revealed the expression of circ_0008037 in transfected NSCLC cells. (c–g) The proliferation, colony formation, migration, and invasion of transfected NSCLC cells were determined by MTT, colony formation, or transwell assays. (h, i) Protein levels of MMP2 and MMP9 in transfected NSCLC cells were assessed by western blotting. * $P < 0.05$

Circ_0008037 silencing repressed proliferation, migration, invasion, and the Warburg effect of NSCLC cells

To further investigate the influence of circ_0008037 on NSCLC progression and glucose metabolism, we synthesized three siRNAs that interfere with circ_0008037 at the junction sites. The transfection efficiency of three siRNAs that interfere with circ_0008037 was shown in Figure S1, and the siRNA targeting circ_0008037 with the strongest interference efficiency was used for subsequent analysis (Figure 2a,b). MTT and colony formation assays presented that circ_0008037 inhibition markedly restrained proliferation and colony formation of NSCLC cells (Figure 2c–e). Transwell assay showed that circ_0008037 knockdown resulted in a significant decrease in the number of migrating and invading NSCLC

cells (Figure 2f,g). Protein levels of MMP2 and MMP9 are used as indicators of migration and invasion.^{27,28} As expected, the protein levels of MMP2 and MMP9 were significantly decreased in si-circ_0008037-transfected NSCLC cells (Figure 2h,i). Next, we explored the influence of circ_0008037 knockdown on the glycolysis of NSCLC cells. The results exhibited that circ_0008037 silencing led to an apparent reduction in lactate production and glucose consumption in NSCLC cells (Figure S2a,b). We further analyzed the impact of circ_0008037 inhibition on ECAR and OCR (a marker of oxidative phosphorylation) through using an XFe 96 Extracellular Flux analyzer. The results presented that circ_0008037 inhibition decreased ECAR but elevated OCR in NSCLC cells (Figure S2c–f). Western blotting exhibited that the protein levels of HK2 and LDHA were repressed in NSCLC cells after circ_0008037 silencing (Figure S2g,h). Together, these

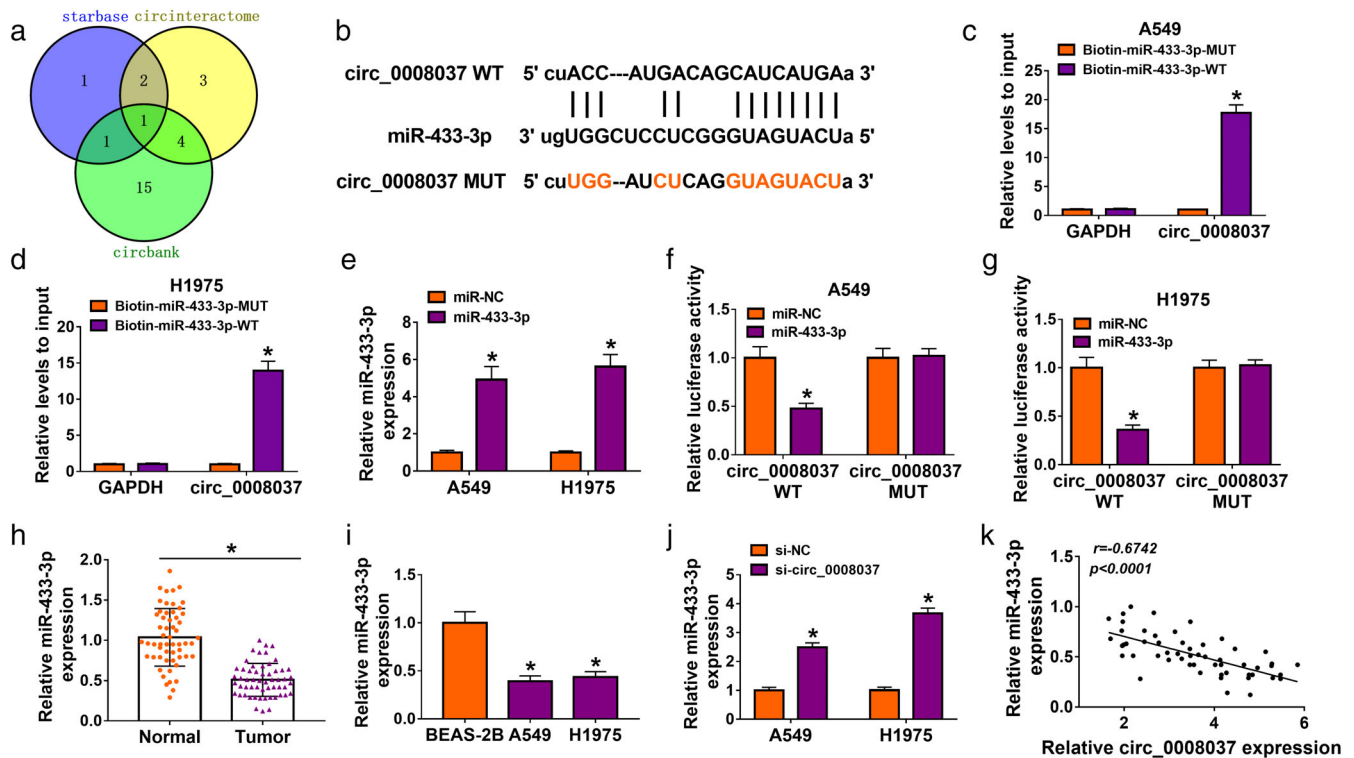


FIGURE 3 Circ_0008037 could interact with miR-433-3p. (a) The binding sites between circ_0008037 and miR-433-3p were jointly predicted by online prediction tools (circinteractome, starbase, and circbank). (b) The alignment of circ_0008037 with miR-433-3p. (c, d) RNA pull-down assay was performed to analyze the relationship between circ_0008037 and miR-433-3p in NSCLC cells. (e) RT-qPCR analysis of miR-433-3p in NSCLC cells transfected with miR-433-3p mimic or miR-NC. (f, g) Dual-luciferase reporter assay was carried out to analyze the luciferase activity of the psiCHECK-2 vector carrying circ_0008037 WT or circ_0008037 MUT in NSCLC cells transfected with miR-NC or miR-433-3p mimic. (h, i) The expression of miR-433-3p in NSCLC tissues and cells was assessed by RT-qPCR. (j) Expression of miR-433-3p in NSCLC cells transfected with si-NC or si-circ_0008037 by RT-qPCR. (k) Correlation between miR-433-3p and circ_0008037 was evaluated by Pearson's correlation analysis. * $P < 0.05$

findings suggested that circ_0008037 facilitated proliferation, migration, invasion, and the Warburg effect of NSCLC cells.

Circ_0008037 could interact with miR-433-3p

Given that circ_0008037 was abundant in the cytoplasm, we further explored the regulatory mechanism of circ_0008037 in NSCLC. Online prediction tools (Circinteractome, StarBase, and Circbank) exhibited that circ_0008037 had potent binding sites for miR-433-3p (Figure 3a,b). RNA pull-down assay presented that circ_0008037 could be pulled down by the Biotin-miR-433-3p-WT probe compared to the Biotin-miR-433-3p-MUT probe (Figure 3c,d). The transfection of miR-433-3p mimic was assessed by RT-qPCR analysis, showing an apparent upregulation of miR-433-3p in NSCLC cells (Figure 3e). Dual-luciferase reporter assay indicated that the luciferase intensity of the psiCHECK-2 vector carrying circ_0008037 WT was repressed in NSCLC cells by miR-433-3p overexpression, but there was no apparent change in the psiCHECK-2 vector carrying circ_0008037 MUT (Figure 3f,g). We then detected miR-433-3p expression in NSCLC tissues and cells, and RT-qPCR displayed that miR-433-3p was apparently downregulated in NSCLC

tissues and cells (Figure 3h,i). In addition, miR-433-3p expression was elevated in si-circ_0008037-transfected NSCLC cells (Figure 3j). Also, the expression of miR-433-3p was negatively correlated with circ_0008037 expression in NSCLC tissues (Figure 3k). Together, these results indicated that circ_0008037 could adsorb miR-433-3p through functioning as a ceRNA in NSCLC.

Circ_0008037 regulated proliferation, migration, invasion, and the Warburg effect of NSCLC cells by sponging miR-433-3p

Based on the above results, we evaluated whether miR-433-3p was involved in circ_0008037-mediated proliferation, migration, invasion, and the Warburg effect of NSCLC cells. The transfection of miR-433-3p inhibitor was detected by RT-qPCR analysis, exhibiting a marked downregulation of miR-433-3p in NSCLC cells (Figure 4a). Rescue experiments presented that miR-433-3p inhibitor reversed the inhibitory influence of circ_0008037 silencing on proliferation, colony formation, migration, and invasion of NSCLC cells (Figure 4b–f). Moreover, the downregulation of MMP2 and MMP9 in si-circ_0008037-transfected NSCLC cells was

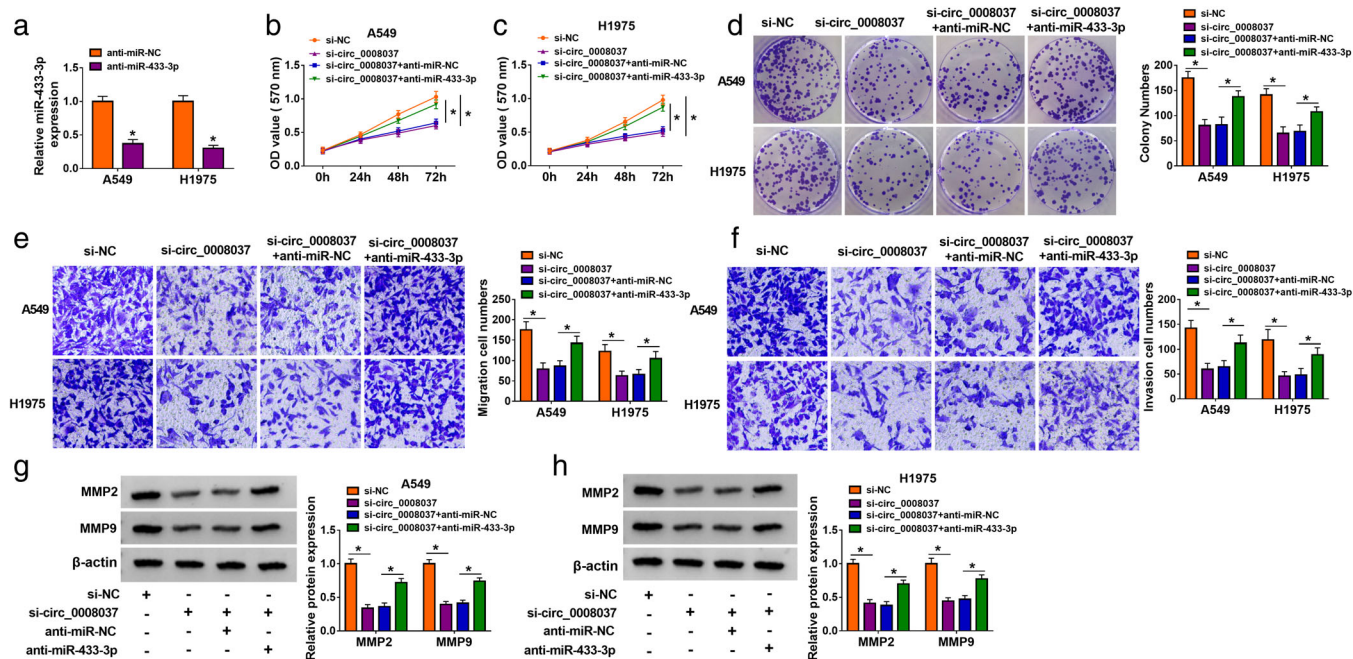


FIGURE 4 Circ_0008037 regulated NSCLC cell proliferation, migration, and invasion via adsorbing miR-433-3p in NSCLC cells. (a) RT-qPCR analysis of miR-433-3p in NSCLC cells transfected with anti-miR-NC or anti-miR-433-3p. (b–h) NSCLC cells were transfected with si-NC, si-circ_0008037, si-circ_0008037 + anti-miR-NC, or si-circ_0008037 + anti-miR-433-3p. (b–f) MTT, colony formation, and transwell assays were executed to evaluate proliferation, colony formation, migration, or invasion of transfected NSCLC cells. (g, h) Western blotting analysis of protein levels of MMP2 and MMP9 in transfected NSCLC cells. * $P < 0.05$

reversed after miR-433-3p inhibitor introduction (Figure 4g, h). Furthermore, silenced miR-433-3p expression rescued the decrease of lactate production and glucose consumption in NSCLC cells mediated by circ_0008037 inhibition (Figure S3a,b). Also, miR-433-3p inhibitor overturned circ_0008037 silencing-mediated effects on ECAR and OCR in NSCLC cells (Figure S3c–f). Additionally, downregulation of miR-433-3p also offset the suppressive effect of circ_0008037 silencing on protein levels of HK2 and LDHA in NSCLC cells (Figure S3g,h). Therefore, these findings indicated that circ_0008037 regulated proliferation, migration, invasion, and the Warburg effect of NSCLC cells via sponging miR-433-3p.

NUCKS1 was identified as a target of miR-433-3p

We then surveyed the latent targets of miR-433-3p. The online prediction tool StarBase showed that NUCKS1 might be a downstream target of miR-433-3p (Figure 5a). Dual-luciferase reporter assay exhibited that miR-433-3p mimic reduced the luciferase activity of the psiCHECK-2 vector carrying NUCKS1 3'-UTR-WT in NSCLC cells, while the luciferase activity of the psiCHECK-2 vector carrying NUCKS1 3'-UTR-MUT did not change (Figure 5b,c). miR-433-3p mimic repressed the mRNA and protein levels of NUCKS1 in NSCLC cells (Figure 5d,e). Moreover, the expression of NUCKS1 mRNA was markedly elevated in

NSCLC tissues relative to the paracarcinoma tissues (Figure 5f). The level of NUCKS1 protein was upregulated in 5 NSCLC tissues in six random samples (Figure 5g). Also, there was a negative correlation between NUCKS1 and miR-433-3p expression in NSCLC tissues (Figure 5h). Analogously, the levels of NUCKS1 mRNA and protein were elevated in NSCLC cells compared with the BEAS-2B cells (Figure 5i,j). In addition, silenced circ_0008037 expression distinctly reduced the levels of NUCKS1 mRNA and protein in NSCLC cells, while this decrease was partly recovered by miR-433-3p inhibition (Figure 5k,l). And the expression of NUCKS1 mRNA was positively correlated with circ_0008037 expression in NSCLC tissues (Figure 5m). Thus, these findings manifested that miR-433-3p targeted NUCKS1, and circ_0008037 modulated NUCKS1 expression through sponging miR-433-3p in NSCLC cells.

MiR-433-3p modulated proliferation, migration, invasion, and the Warburg effect of NSCLC cells by targeting NUCKS1

Considering the targeting relationship between miR-433-3p and NUCKS1 in NSCLC cells, we analyzed whether miR-433-3p regulated proliferation, migration, invasion, and the Warburg effect of NSCLC cells via NUCKS1. The level of NUCKS1 protein was elevated in NSCLC cells after transfection with the NUCKS1 overexpression plasmid (Figure 6a). Moreover, we observed that forced NUCKS1 expression

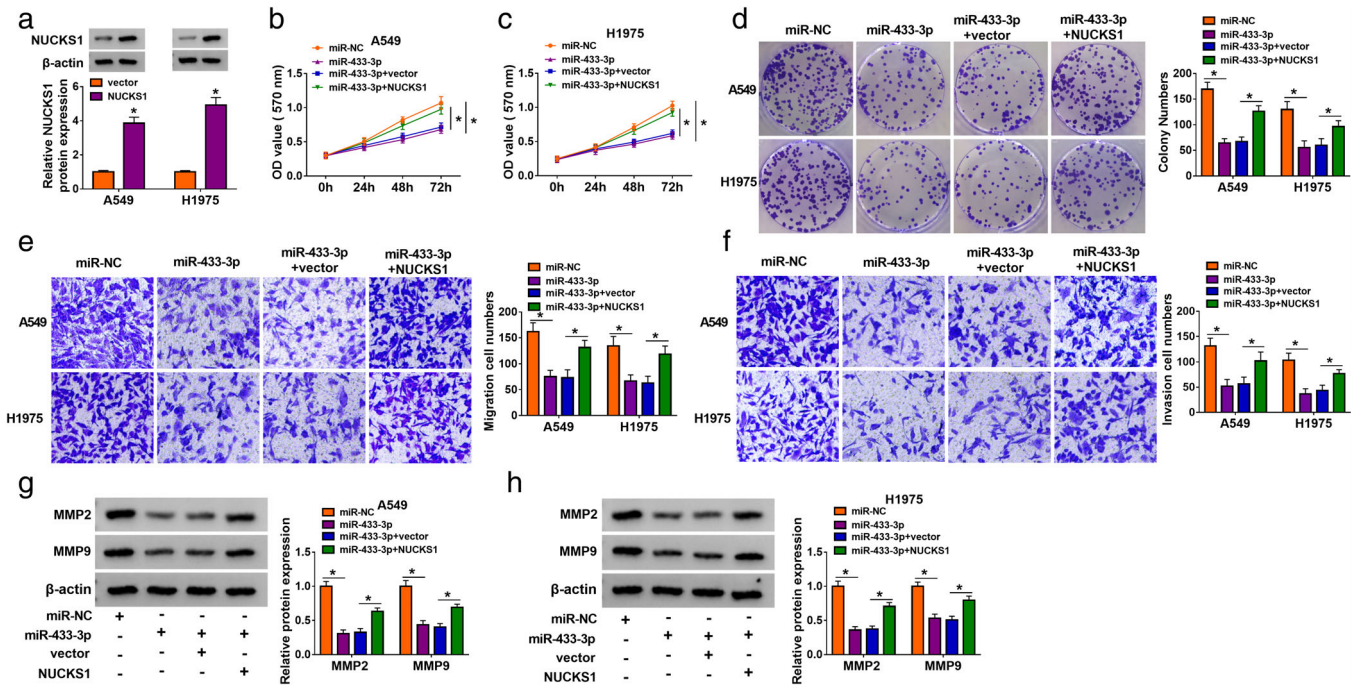


FIGURE 6 MiR-433-3p regulated NSCLC cell proliferation, migration, and invasion via targeting NUCKS1. (a) Level of NUCKS1 protein in NSCLC cells transfected with vector or NUCKS1 was detected by western blotting. (b–h) NSCLC cells were transfected with miR-NC, miR-433-3p, miR-433-3p + vector, or miR-433-3p + NUCKS1. (b–f) The proliferation, colony formation, migration, and invasion of transfected NSCLC cells were analyzed by using MTT, colony formation, or transwell assays. (g, h) Levels of MMP2 and MMP9 in transfected NSCLC cells were detected by western blotting. * $P < 0.05$

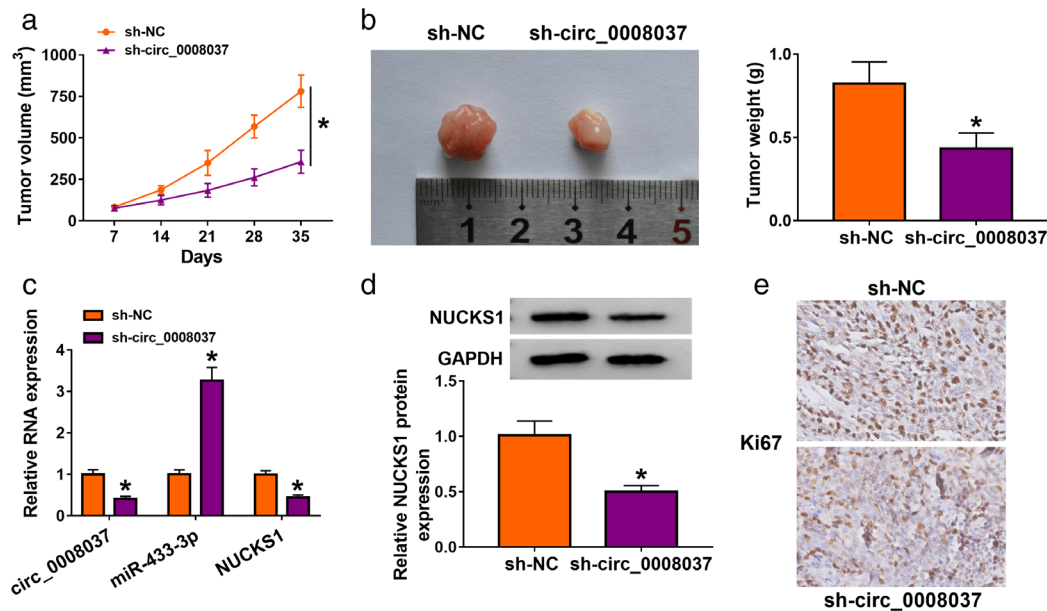


FIGURE 7 Circ_0008037 silencing decreased NSCLC growth in vivo. (a) Tumor volume was monitored once a week with a digital caliper. (b) Analysis of tumor weight in sh-circ_0008037 or sh-NC groups. (c, d) The levels of circ_0008037, miR-433-3p, NUCKS1 were analyzed by RT-qPCR or western blotting. (e) IHC analysis of Ki67 in tumor tissues in sh-circ_0008037 or sh-NC groups. * $P < 0.05$

of HK2 and LDHA in miR-433-3p-overexpressed NSCLC cells (Figure S4g,h). These results manifested that miR-433-3p regulated proliferation, migration, invasion, and the Warburg effect of NSCLC cells via targeting NUCKS1.

Silencing of circ_0008037 decreased tumor growth in vivo

To verify the oncogenicity of circ_0008037 in NSCLC in vivo, we constructed the xenograft mouse models through

injecting A549 cells stably expressing sh-circ_0008037 or sh-NC into nude mice. In comparison to the control group, tumor volume and weight were smaller and lighter in the sh-circ_0008037 group (Figure 7a,b). Also, the expression of circ_0008037 and NUCKS1 were reduced in xenograft tissues in the circ_0008037 group compared to the control group, but miR-433-3p expression had an opposing result (Figure 7c,d). Also, the number of Ki67-positive cells was less in sh-circ_0008037 group with respect to the sh-NC group (Figure 7e). These data indicated that circ_0008037 silencing could decrease NSCLC growth in vivo.

DISCUSSION

Recent studies have proved that circRNAs play crucial roles in tumor occurrence and advancement, including NSCLC.²⁹ For instance, circRNA circBIRC6,³⁰ circRNA circFOXM1,³¹ and circRNA circSOX4³² have been shown to play a cancerogenic role in NSCLC, but circRNA circ_0011780³³ and circRNA circLARP4³⁴ exert a repressive role in NSCLC. Herein, circ_0008037 was overexpressed in NSCLC. Moreover, NSCLC patients with high circ_0008037 expression had a poor prognosis, illustrating that circ_0008037 might be a prognostic biomarker for NSCLC patients. In addition, circ_0008037 silencing repressed xenograft tumor growth in vivo and decreased NSCLC cell Warburg effect, restrained NSCLC cell proliferation, migration, and invasion in vitro. The Warburg effect mainly provides energy for the tumor microenvironment,³⁵ and is also involved in cancer cell invasion and proliferation.³⁶ Thus, we concluded that circ_0008037 exerts a promoting influence on tumor growth and the Warburg effect in NSCLC.

CircRNAs can participate in NSCLC progression through functioning as ceRNAs via adsorbing miRs.³⁷ Through online prediction and experimental validation, circ_0008037 was confirmed as a miR-433-3p decoy. Furthermore, miR-433-3p downregulation counteracted circ_0008037 silencing-mediated effects on NSCLC cell proliferation, migration, invasion, and the Warburg effect. The study by Zhang et al. manifested that hsa_circ_0010235 downregulation facilitated NSCLC cell apoptosis and repressed NSCLC cell autophagy and proliferation by decreasing TIPRL expression via releasing miR-433-3p.¹⁷ Also, circMED13L_012 elevated MAPK8 expression through adsorbing miR-433-3p, thus elevating cell chemoresistance and promoting metastasis and invasion in NSCLC.¹⁶ Accordingly, we inferred that circ_0008037 regulated NSCLC cell proliferation, migration, invasion, and the Warburg effect through adsorbing miR-433-3p.

Subsequently, NUCKS1 as a target for miR-433-3p was validated. A previous study uncovered that NUCKS1 upregulation was related to recurrence, lymph node metastasis, deep stromal infiltration, and poor histological grade of cervical squamous cell carcinoma patients.³⁸ NUCKS1 could activate the PI3K/AKT/mTOR pathway via elevating IGF-1R expression, thereby facilitating cell aggressiveness in gastric cancer.²¹ Also, NUCKS1 upregulation was related to

a poor prognosis of lung adenocarcinoma patients.³⁹ Furthermore, NUCKS1 elevation interacted with CDK1, thereby accelerating tumor growth in NSCLC.²³ Herein, NUCKS1 was upregulated in NSCLC, and NUCKS1 upregulation offset the inhibiting impact of miR-433-3p elevation on NSCLC cell proliferation, migration, invasion, and the Warburg effect. Importantly, circ_0008037 could regulate NUCKS1 expression by adsorbing miR-433-3p. Thus, we concluded that circ_0008037 regulated NSCLC progression and the Warburg effect via modulating the miR-433-3p/NUCKS1 axis.

In summary, circ_0008037 elevated the Warburg effect and accelerated tumor growth via upregulating NUCKS1 through acting as a miR-433-3p decoy in NSCLC. This study provides a new mechanism by which circ_0008037 was responsible for the Warburg effect and tumor growth in NSCLC.

CONFLICT OF INTEREST

The authors declare that they have no financial conflicts of interest.

ORCID

Yang Sun  <https://orcid.org/0000-0001-8987-9231>

REFERENCES

1. Bray F, Ferlay J, Soerjomataram I, Siegel RL, Torre LA, Jemal A. Global cancer statistics 2018: GLOBOCAN estimates of incidence and mortality worldwide for 36 cancers in 185 countries. *CA Cancer J Clin.* 2018;68(6):394–424.
2. Herbst RS, Morgensztern D, Boshoff C. The biology and management of non-small cell lung cancer. *Nature.* 2018;553(7689):446–54.
3. Siegel RL, Miller KD, Jemal A. Cancer statistics, 2018. *CA Cancer J Clin.* 2018;68(1):7–30.
4. Bhattacharya B, Mohd Omar MF, Soong R. The Warburg effect and drug resistance. *Br J Pharmacol.* 2016;173(6):970–9.
5. Schwartz L, Seyfried T, Alfarouk KO, Da Veiga MJ, Fais S. Out of Warburg effect: an effective cancer treatment targeting the tumor specific metabolism and dysregulated pH. *Semin Cancer Biol.* 2017;43:134–8.
6. de la Cruz-López KG, Castro-Muñoz LJ, Reyes-Hernández DO, García-Carrancá A, Manzo-Merino J. Lactate in the regulation of tumor microenvironment and therapeutic approaches. *Front Oncol.* 2019;9:1143.
7. Salzman J, Gawad C, Wang PL, Lacayo N, Brown PO. Circular RNAs are the predominant transcript isoform from hundreds of human genes in diverse cell types. *PLoS One.* 2012;7(2):e30733.
8. Qu S, Yang X, Li X, Wang J, Gao Y, Shang R, et al. Circular RNA: a new star of noncoding RNAs. *Cancer Lett.* 2015;365(2):141–8.
9. Rybak-Wolf A, Stottmeister C, Glažar P, Jens M, Pino N, Giusti S, et al. Circular RNAs in the mammalian brain are highly abundant, conserved, and dynamically expressed. *Mol Cell.* 2015;58(5):870–85.
10. Song X, Liang Y, Sang Y, Li Y, Zhang H, Chen B, et al. circHMCU promotes proliferation and metastasis of breast cancer by sponging the let-7 family. *Mol Ther Nucleic Acids.* 2020;20:518–33.
11. Mishra S, Yadav T, Rani V. Exploring miRNA based approaches in cancer diagnostics and therapeutics. *Crit Rev Oncol Hematol.* 2016;98:12–23.
12. Rupaimoole R, Slack FJ. MicroRNA therapeutics: towards a new era for the management of cancer and other diseases. *Nat Rev Drug Discov.* 2017;16(3):203–22.

13. Lei B, Wang D, Zhang M, Deng Y, Jiang H, Li Y. miR-615-3p promotes the epithelial-mesenchymal transition and metastasis of breast cancer by targeting PICK1/TGFBR1 axis. *J Exp Clin Cancer Res.* 2020;39(1):71.
14. Liu J, Jia Y, Jia L, Li T, Yang L, Zhang G. MicroRNA 615-3p inhibits the tumor growth and metastasis of NSCLC via inhibiting IGF2. *Oncol Res.* 2019;27(2):269–79.
15. Liu X, Huang S, Guan Y, Zhang Q. Long noncoding RNA OSER1-AS1 promotes the malignant properties of non-small cell lung cancer by sponging microRNA-433-3p and thereby increasing Smad2 expression. *Cancer Cell Int.* 2020;44(2):599–610.
16. Chen W, Zheng G, Huang J, Zhu L, Li W, Guo T, et al. CircMED13L_012 promotes lung adenocarcinoma progression by upregulation of MAPK8 mediated by miR-433-3p. *Cancer Cell Int.* 2021;21(1):111.
17. Zhang F, Cheng R, Li P, Lu C, Zhang G. Hsa_circ_0010235 functions as an oncogenic drive in non-small cell lung cancer by modulating miR-433-3p/TIPRL axis. *Cancer Cell Int.* 2021;21(1):73.
18. Maranon DG, Sharma N, Huang Y, Selemenakis P, Wang M, Altina N, et al. NUCKS1 promotes RAD54 activity in homologous recombination DNA repair. *J Cell Biol.* 2020;219(10):e201911049.
19. Qiu B, Han W, Tergaonkar V. NUCKS: a potential biomarker in cancer and metabolic disease. *Clin Sci.* 2015;128(10):715–21.
20. Kikuchi A, Ishikawa T, Mogushi K, Ishiguro M, Iida S, Mizushima H, et al. Identification of NUCKS1 as a colorectal cancer prognostic marker through integrated expression and copy number analysis. *Int J Cancer.* 2013;132(10):2295–302.
21. Huang YK, Kang WM, Ma ZQ, Liu YQ, Zhou L, Yu JC. NUCKS1 promotes gastric cancer cell aggressiveness by upregulating IGF-1R and subsequently activating the PI3K/Akt/mTOR signaling pathway. *Carcinogenesis.* 2019;40(2):370–9.
22. Cheong JY, Kim YB, Woo JH, Kim DK, Yeo M, Yang SJ, et al. Identification of NUCKS1 as a putative oncogene and immunodiagnostic marker of hepatocellular carcinoma. *Gene.* 2016;584(1):47–53.
23. Zhao S, Wang B, Ma Y, Kuang J, Liang J, Yuan Y. NUCKS1 promotes proliferation, invasion and migration of non-small cell lung cancer by upregulating CDK1 expression. *Cancer Manag Res.* 2020;12:13311–23.
24. Jiang B, Fan X, Zhang D, Liu H, Fan C. Identifying UBA2 as a proliferation and cell cycle regulator in lung cancer A549 cells. *J Cell Biochem.* 2019;120(8):12752–61.
25. Zhang S, Cheng J, Quan C, Wen H, Feng Z, Hu Q, et al. circCELSR1 (hsa_circ_0063809) contributes to paclitaxel resistance of ovarian cancer cells by regulating FOXR2 expression via miR-1252. *Mol Ther Nucleic Acids.* 2020;19:718–30.
26. Zhai W, Zhu R, Ma J, Gong D, Zhang H, Zhang J, et al. A positive feed-forward loop between LncRNA-URRCC and EGFL7/P-AKT/FOXO3 signaling promotes proliferation and metastasis of clear cell renal cell carcinoma. *Mol Cancer.* 2019;18(1):81.
27. Jacob A, Prekeris R. The regulation of MMP targeting to invadopodia during cancer metastasis. *Front Cell Dev Biol.* 2015;3:4.
28. Shay G, Lynch CC, Fingleton B. Moving targets: emerging roles for MMPs in cancer progression and metastasis. *Matrix Biol.* 2015;44–46:200–6.
29. Wang Y, Mo Y, Gong Z, Yang X, Yang M, Zhang S, et al. Circular RNAs in human cancer. *Mol Cancer.* 2017;16(1):25.
30. Yang H, Zhao M, Zhao L, Li P, Duan Y, Li G. CircRNA BIRC6 promotes non-small cell lung cancer cell progression by sponging microRNA-145. *Cell Oncol (Dordr).* 2020;43(3):477–88.
31. Yu C, Cheng Z, Cui S, Mao X, Li B, Fu Y, et al. circFOXM1 promotes proliferation of non-small cell lung carcinoma cells by acting as a ceRNA to upregulate FAM83D. *J Exp Clin Cancer Res.* 2020;39(1):55.
32. Wang L, Zheng C, Wu X, Zhang Y, Yan S, Ruan L, et al. Circ-SOX4 promotes non-small cell lung cancer progression by activating the Wnt/beta-catenin pathway. *Mol Oncol.* 2020;14(12):3253.
33. Liu Y, Yang C, Cao C, Li Q, Jin X, Shi H. Hsa_circ_RNA_0011780 represses the proliferation and metastasis of non-small cell lung cancer by decreasing FBXW7 via targeting miR-544a. *Onco Targets Ther.* 2020;13:745–55.
34. Shi JQ, Wang B, Cao XQ, Wang YX, Cheng X, Jia CL, et al. Circular RNA_LARP4 inhibits the progression of non-small-cell lung cancer by regulating the expression of SMAD7. *Eur Rev Med Pharmacol Sci.* 2020;24(4):1863–9.
35. Vander Heiden MG, Cantley LC, Thompson CB. Understanding the Warburg effect: the metabolic requirements of cell proliferation. *Science.* 2009;324(5930):1029–33.
36. Icard P, Shulman S, Farhat D, Steyaert J-M, Alifano M, Lincet H. How the Warburg effect supports aggressiveness and drug resistance of cancer cells? *Drug Resist Updat.* 2018;38:1–11.
37. Tang X, Ren H, Guo M, Qian J, Yang Y, Gu C. Review on circular RNAs and new insights into their roles in cancer. *Comput Struct Biotechnol J.* 2021;19:910–28.
38. Gu L, Xia B, Zhong L, Ma Y, Liu L, Yang L, et al. NUCKS1 overexpression is a novel biomarker for recurrence-free survival in cervical squamous cell carcinoma. *Tumour Biol.* 2014;35(8):7831–6.
39. Ma H, Xu J, Zhao R, Qi Y, Ji Y, Ma K. Upregulation of NUCKS1 in lung adenocarcinoma is associated with a poor prognosis. *Cancer Invest.* 2021;39(5):435–44.

SUPPORTING INFORMATION

Additional supporting information may be found in the online version of the article at the publisher's website.

How to cite this article: Yu J, Zhang H, Zhao C, Li G, Zhang Y, Sun Y. CircRNA circ_0008037 facilitates tumor growth and the Warburg effect via upregulating NUCKS1 by binding to miR-433-3p in non-small cell lung cancer. *Thorac Cancer.* 2022;13:162–72. <https://doi.org/10.1111/1759-7714.14235>